

Secondary laser cooling and capturing of thulium atoms in traps

D.D. Sukachev, E.S. Kalganova, A.V. Sokolov, S.A. Fedorov, G.A. Vishnyakova, A.V. Akimov, N.N. Kolachevsky, V.N. Sorokin

Abstract. Secondary laser cooling has been realised on the weak dipole transition $4f^{13}(^2F^{\circ})6s^2, J = 7/2, F = 4 \rightarrow 4f^{12}(^3H_6)5d_{5/2}6s^2, J' = 9/2, F' = 5$ with the wavelength of 530.7 nm and natural width of 350 kHz. The temperature of the atomic cloud in a magneto-optical trap (MOT) was 30 μ K at the lifetime of 2 s and the number of atoms 10^5 . Approximately 1% of atoms from the MOT have been reloaded to an optical dipole trap and to one-dimensional optical lattice at the wavelength of 532 nm. The atom lifetime in the optical lattice was 320 ms. We propose to employ thulium atoms captured in an optical lattice as an optical frequency reference.

Keywords: laser cooling, rare-earth atoms, thulium, dipole trap, optical lattice, frequency standards.

1. Introduction

At present, laser cooling [1] and capturing of neutral atoms in traps [2] is the most popular method for obtaining and studying ultra-cold atoms [3]. Ensembles of ultra-cold atoms are employed in precision laser spectroscopy [4], investigation of atomic collisions [5], atomic interferometers [6], and for creating quantum-degenerated systems [7]. Laser-cooled atoms and ions are used for constructing optical frequency standards [4], which in many aspects are superior to microwave

standards [8]. Most convenient objects for studying metrological transitions are atoms captured in an optical lattice [9]. In that case, the shift and broadening of the line of metrological transition caused by interaction between atoms can be minimised, and the Doppler broadening can be suppressed by localising an atom in a spatial domain of size less than the wavelength of the transition under study (Lamb–Dicke effect [10]). However, laser radiation which produces an optical lattice shifts the frequency of the metrological transition due to a dynamic Stark effect. Nevertheless, one may choose the wavelength of the radiation used for creating the optical lattice such that the dynamic shifts of levels of metrological transition would coincide in a linear approximation; this will result in a minimal frequency shift of this transition [11]. For example, the relative instability of the optical frequency standard on Yb atoms captured in the optical lattice was 10^{-18} [12].

We suggest employment of the forbidden magneto-dipole transition between components of the fine structure of a ground state in thulium atoms (see Fig. 1) with the wavelength of 1.14 μ m and natural width of ~ 1 Hz [13] as a frequency reference [14]. Due to the specific features of the electron structure of thulium atoms the dynamic polarisabilities of lower and upper levels of the metrological transition have close values [15]. This stipulates suppression of the dynamic Stark frequency shift of the metrological transition in a wide range of wavelengths of the laser radiation which forms the optical potential.

In metrological measurements it is customary to employ optical lattices of depth of about 10 μ K. In order to efficiently load atoms in such an optical lattice they should have a temperature of at most 10 μ K. Although the primary laser cooling on a strong transition may provide a temperature of about 30 μ K [16, 17] due to the sub-Doppler mechanism of cooling [18], obtaining such temperatures requires a thorough adjustment of cooling beams and is accompanied by a reduction of the number of captured atoms. Secondary laser cooling on a weak transition with a lower Doppler limitation gives a chance to lower the temperature of atoms without a substantial reduction in the number of atoms [19].

In spite of a complicated structure of levels of rare-earth elements, much success has been achieved in the recent decade in the field of laser cooling of lanthanides (Er [20], Dy [21], Ho [22], Tm [23]). The present work is aimed at studying secondary laser cooling of thulium atoms on the transition $4f^{13}(^2F^{\circ})6s^2, J = 7/2, F = 4 \rightarrow 4f^{12}(^3H_6)5d_{5/2}6s^2, J' = 9/2, F' = 5$ with the wavelength of 530.7 nm and at the possibility of capturing cold thulium atoms in an optical dipole trap (and in an optical lattice) at the wavelength of 532 nm.

D.D. Sukachev, V.N. Sorokin P.N. Lebedev Physics Institute, Russian Academy of Sciences, Leninsky prosp. 53, 119991 Moscow, Russia; Russian Quantum Centre, Business Centre 'URAL', ul. Novaya 100A, 143025 Skolkovo, Odintsovo district, Moscow region, Russia; e-mail: sukachev@gmail.com, sovni@lebedev.ru;

E.S. Kalganova, G.A. Vishnyakova, A.V. Akimov, N.N. Kolachevsky P.N. Lebedev Physics Institute, Russian Academy of Sciences, Leninsky prosp. 53, 119991 Moscow, Russia; Moscow Institute of Physics and Technology, Institutskii per. 9, 141700 Dolgoprudnyi, Moscow region, Russia; Russian Quantum Centre, Business Centre 'URAL', ul. Novaya 100A, 143025 Skolkovo, Odintsovo district, Moscow region, Russia; e-mail: Kalganova.elena@gmail.com, AkimovWork@mail.ru, kolachbox@mail.ru, gulnarav7@gmail.com;

A.V. Sokolov P.N. Lebedev Physics Institute, Russian Academy of Sciences, Leninsky prosp. 53, 119991 Moscow, Russia; e-mail: teopetuk@gmail.com;

S.A. Fedorov P.N. Lebedev Physics Institute, Russian Academy of Sciences, Leninsky prosp. 53, 119991 Moscow, Russia; Moscow Institute of Physics and Technology, Institutskii per. 9, 141700 Dolgoprudnyi, Moscow region, Russia; e-mail: edorov.s.a@outlook.com

Received 28 January 2014; revision received 3 March 2014

Kvantovaya Elektronika 44 (6) 515–520 (2014)

Translated by N.A. Raspopov

2. Laser cooling

The levels of thulium atoms participating in laser cooling are schematically shown in Fig. 1. For a Zeeman slower [24] and primary laser cooling [17, 23], the strong dipole transition at the wavelength of 410.6 nm with the natural line width $\gamma_{\text{blue}} = 10$ MHz and the corresponding Doppler limit 240 μK is used. The laser radiation at the wavelength of 410.6 nm was produced by frequency doubling (Coherent, MBD-200) a single-frequency MBR-110 Ti:sapphire laser (Coherent) pumped by a semiconductor Verdi G-12 laser (Coherent). Such a laser system provides the output power of 60–100 mW with the spectral linewidth of less than 1 MHz.

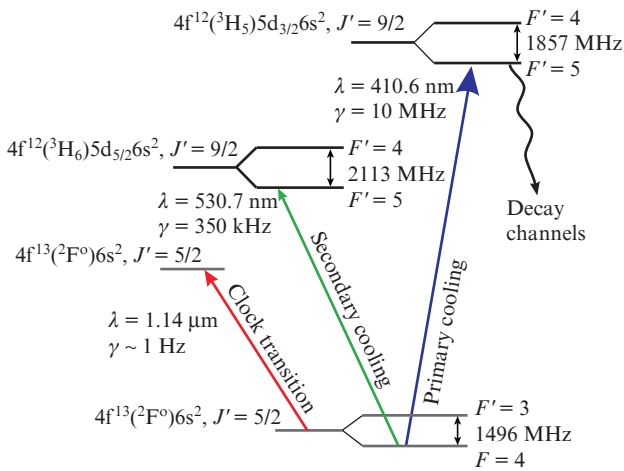


Figure 1. Energy levels of thulium atom. The metrological (clock) transition and transitions used for primary and secondary laser cooling are marked.

Secondary laser cooling of thulium atoms was performed on the weak transition $4f^{13}(^2F^{\circ})6s^2, J = 7/2, F = 4 \rightarrow 4f^{12}(^3H_6)5d_{5/2}6s^2, J' = 9/2, F' = 5$ with the wavelength of 530.7 nm and natural linewidth $\gamma_{\text{green}} = 350$ kHz [25]. The corresponding Doppler limit of the temperature is $T_D = h\gamma_{\text{green}}/2k_B = 9 \mu\text{K}$, where h is Planck's constant and k_B is the Boltzmann constant. The second harmonic of a DL-Pro (Toptica) semiconductor laser with an external resonator power of 50 mW was used for secondary laser cooling.

Frequencies of the both lasers were stabilised by the method of saturated absorption in counterpropagating beams [26] in a cell with thulium vapours. Although the probabilities of cooling transitions and, hence, the absorption rates of thulium vapour for these two transitions substantially differ, it is possible to simultaneously obtain admissible signals of saturated absorption for the both cooling transitions in a single cell at a temperature of $\sim 700^\circ\text{C}$, which corresponds to a pressure of thulium vapour of $\sim 10^{-3}$ mbar [27].

3. Experimental setup

The source of thulium atoms is a sapphire evaporation oven in which metallic thulium is sublimated at a temperature of $700\text{--}900^\circ\text{C}$. The velocities of atoms in a produced atomic beam are reduced in a Zeeman slower to approximately 30 m s^{-1} [28]. To reduce loss of atoms due to a divergence of the atomic beam we used two-dimensional optical molasses which collimated the atomic beam and increased thrice the number of atoms in the primary magneto-optical trap (MOT) that operated at the wavelength of 410.6 nm [29].

The primary and secondary MOTs used a classical configuration comprising a quadruple magnetic field and three mutually orthogonal pairs of the antiparallel beams of laser radiation with circular polarisations and the frequencies lower than that of the cooling transition [2]. Prior to entering the vacuum chamber, the laser beams creating primary and secondary MOTs were spatially matched by a dichroic mirror. A schematic of experimental setup is presented in Fig. 2. A diameter of the beams in the secondary MOT was 5 mm at the $1/e^2$ level and the power of each of six beams was up to 2 mW. This corresponds to a total intensity at the MOT centre of $\sim 15 \text{ mW cm}^{-2}$ (the saturated intensity is $I_0 = 0.3 \text{ mW cm}^{-2}$). The frequency detuning of cooling beams varied from -0.5 to -30 MHz relative to the frequency of the cooling transition at the wavelength of 530.7 nm.

All the laser beams passed through acousto-optical modulators (AOMs) which made it possible to independently control their frequencies and quickly trigger the radiation in a time interval of $\sim 1 \mu\text{s}$.

For controlling the concentration of the cold atoms, the cloud was illuminated by a pulse of probe radiation having a frequency adjusted in resonance with that of the cooling transition at the wavelength of 410.6 nm. Luminescence from the cloud was detected by a photomultiplier tube (PMT) and a CCD-camera (the solid angle of radiation acquisition ~ 0.01 sr).

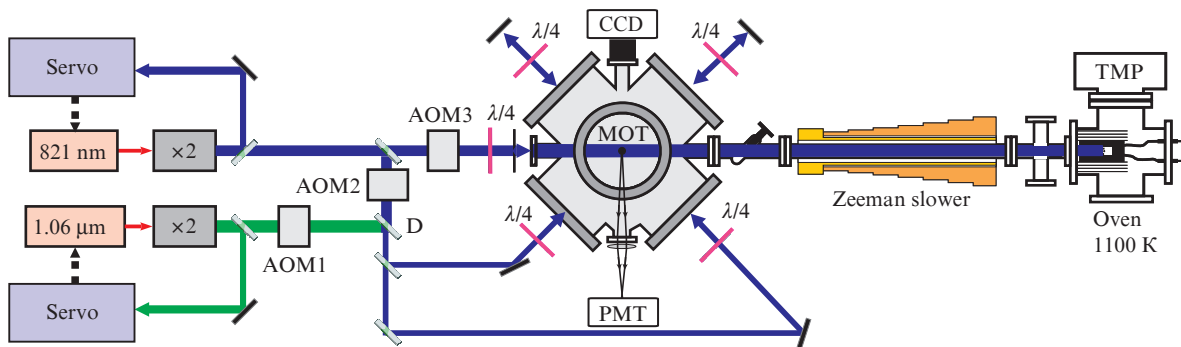


Figure 2. Schematic of experimental the setup [(TMP) turbo-molecular pump; (Servo) system for frequency stabilisation of laser radiation (comprises a scheme of saturated absorption in a separate cell and controlling electronics); (D) dichroic mirror; ($\lambda/4$) quarter-wave phase plates for the wavelengths 410.6 and 530.7 nm; the vertical beam of the MOT is not shown].

4. Loading of a secondary MOT

Atoms may be loaded to a secondary MOT in two ways: by reloading atoms from a primary MOT or by a direct capture of atoms from the atomic beam. The limiting velocity of atoms at which they may be captured to the secondary MOT (the capture velocity) for the parameters of our setup is $3\text{--}5\text{ m s}^{-1}$. The average velocity of atoms in the primary MOT is noticeably lower; hence, atoms are reloaded from the primary to the secondary MOT at actually 100% efficiency. We also realised the direct loading of the secondary MOT from the atomic beam. By comparing the capture velocity to the secondary MOT and the average velocity of decelerated atoms in the beam ($20\text{--}30\text{ m s}^{-1}$) one may assume that in this case the number of atoms in the secondary MOT will be noticeably smaller than in the primary. However, the lifetime of atoms in the secondary MOT is by an order of magnitude longer than in the primary MOT and the number of captured atoms is proportional to the lifetime (see below). Hence, the secondary MOT can be efficiently loaded directly from the atomic beam. Note that loading is efficient only at a high power of cooling radiation ($I > 10I_0$) and large frequency detunings ($\delta \approx -10\gamma_{\text{green}}$). Depending on the evaporation oven temperature and on the frequencies and intensities of radiation of cooling laser beams, the number of atoms in the secondary MOT was $10^4\text{--}10^6$ [17, 23].

5. Atom lifetime in the secondary MOT

The kinetics of the number of atoms N in the MOT is described by the equation:

$$\frac{dN}{dt} = R - \frac{N}{\tau} - \beta N^2, \quad (1)$$

where R is the number of captured atoms per second; τ is the lifetime determined by the losses which are linear in N ; and β is the coefficient responsible for the losses of atoms from MOT which are quadratic in N . If, in a fully loaded trap, the radiation passing to the Zeeman slower is switched off then the capture of new atoms stops ($R = 0$) and the population of trap begin to fall. In the case where binary collisions are neglected the population of the MOT falls according to the exponential law:

$$N(t) = N_0 \exp(-t/\tau). \quad (2)$$

The kinetics of the number of atoms in the secondary MOT was measured in the following way. As the trap is fully loaded, the radiation passing to the Zeeman slower is blocked; the magnetic field and laser beams in the MOT are still switched on. Then the cloud of cold atoms is illuminated by a periodic series of radiation pulses of the probe laser matched in resonance with the primary cooling transition at the wavelength of 410.6 nm. The luminescence of atoms is detected by the PMT in front of which an interference filter is placed for transmitting the corresponding spectral part. The duty factor of the pulses of the probe laser is chosen so that an influence of the non-cyclic character of the primary cooling transition is excluded [23]. A typical curve of the MOT population decay is shown in Fig. 3. The lifetime of atoms in the trap amounted to $2.0 \pm 0.1\text{ s}$.

The lifetime of thulium atoms in the secondary MOT is determined by the following factors: collisions with residual gases, collisions with atoms from the atomic beam, optical

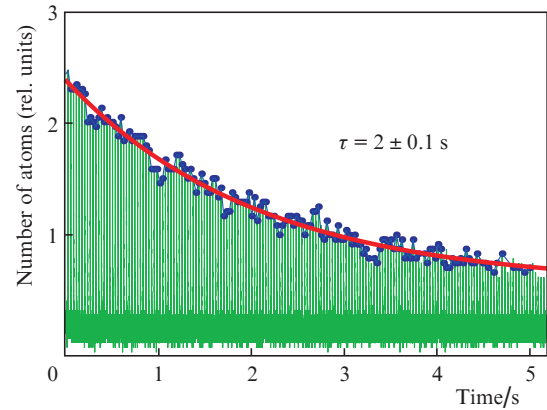


Figure 3. Kinetics of the number of atoms in the secondary MOT after blocking the radiation passing to the Zeeman slower.

pumping to the sublevel $F = 3$ of the ground state, and binary collisions of thulium atoms captured in the MOT. Since the number of atoms in the MOT falls exponentially (see Fig. 3) the role of binary collisions is negligible (otherwise the dependence would be substantially nonexponential). By varying the atomic flow from the Zeeman slower it was found that collisions with atoms from the beam are also inessential.

In order to estimate the rate of optical pumping to the sublevel $F = 3$ of the ground state through nonresonance excitation by the cooling radiation of the $F = 4 \rightarrow F' = 4$ transition, a system of optical Bloch equations has been solved [30]. In the calculation, hyperfine components of the ground and excited $[4f^{12}(^3\text{H}_6)5d_{5/2}6s^2, J' = 9/2]$ states have been taken into account. The magnetic structure of levels was ignored. If we assume that the atom at the sublevel $F = 3$ of the ground state leaves the MOT because it actually no more interacts with the cooling radiation than the population of this sublevel will vary exponentially:

$$\rho_{F=3} = 1 - \exp(-t/t_0), \quad (3)$$

$$t_0 = 8 \frac{\Gamma_{4 \rightarrow 5}^2/4 + (2\pi\Delta_2)^2}{s_0\Gamma_{4 \rightarrow 5}^3} \frac{\Gamma_{4 \rightarrow 5}}{\Gamma_{4 \rightarrow 4}},$$

where $\Gamma_{4 \rightarrow 5} = 2\pi \times 350\text{ s}^{-1}$; $\Gamma_{4 \rightarrow 4} \approx \Gamma_{4 \rightarrow 5}/40$ are the probabilities for the $F = 4 \rightarrow F' = 5$ and $F = 4 \rightarrow F' = 4$ transitions, respectively; $\Delta_2 = 2113\text{ MHz}$ is the hyperfine splitting of upper level of the cooling transition [31]; and s_0 is the saturation parameter for the cooling transition. In the experiment, the saturation parameter was $s_0 < 100$; hence, $t_0 \approx 50\text{ s}$. This time is much longer than the measured lifetime for thulium atom in the second MOT; hence, the optical pumping to the sublevel $F = 3$ of the ground state may be neglected.

Thus, the lifetime of atoms in the secondary MOT is determined by collisions with residual gases in a vacuum chamber (a pressure in the chamber is less than $5 \times 10^{-9}\text{ bar}$).

6. Temperature of atoms in the secondary MOT

The temperature of atoms in the MOT was measured by the ballistic expansion method [17]. At a fully loaded MOT all laser beams in the vacuum chamber are switched off (by AOMs). In this case the force, which keeps atoms, vanishes, and the cloud starts expanding. In a time interval Δt (expan-

sion time) the cloud is illuminated by a short-duration pulse of probe radiation at a frequency matched in resonance with the frequency of the primary cooling transition at the wavelength of 410.6 nm. Fluorescence of atoms is detected by a CCD-camera. Then the procedure is repeated for the other time interval Δt . The photographs of the cloud taken in a series of time intervals Δt are shown in Fig. 4. If the initial spatial profile of the atomic concentration in the cloud is described by a Gaussian function, then it remains Gaussian in the course of expansion and its diameter depends on the expansion time as

$$\sigma_{1/e^2} = \sqrt{\sigma_0^2 + \frac{4k_B T}{m} (\Delta t)^2}, \quad (4)$$

where σ_{1/e^2} is the radius of the cloud at the $1/e^2$ level; σ_0 is the initial radius of cloud; m is the atomic mass; k_B is the Boltzmann constant; T is the temperature which we are interested in; and Δt is the time of expansion.

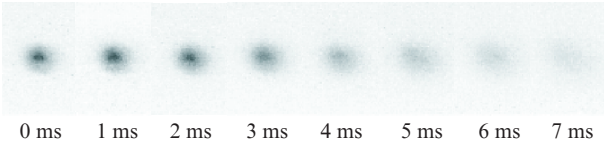


Figure 4. Ballistic expansion of the cloud of thulium atoms from the secondary MOT after switching off all laser beams and the quadruple magnetic field. Time of expansion Δt is pointed.

By approximating the obtained dependence of radius on the expansion time by formula (4) we determined the temperature of atoms in the initial cloud. The dependence of the atom temperature in the secondary MOT on the frequency detuning of cooling radiation is presented in Fig. 5. A minimal obtained temperature was $35 \pm 5 \mu\text{K}$, which is substantially greater than the Doppler limit of $9 \mu\text{K}$. We assume that this excess is related to the fact that the Doppler limit is attained at the frequency detuning of cooling radiation $\gamma_{\text{green}}/2 \approx -175 \text{ kHz}$, whereas the spectral width of second harmonic radiation from a semiconductor laser with an external resonator may be noticeably greater ($\sim 1 \text{ MHz}$), which

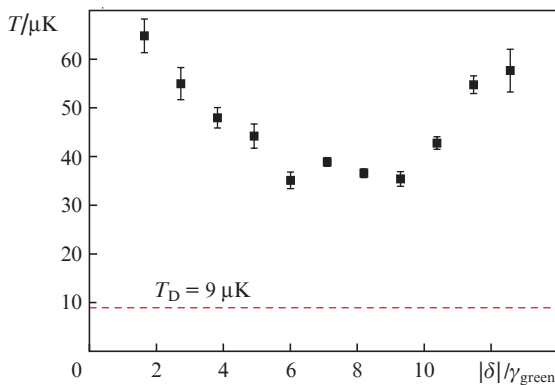


Figure 5. Dependence of the atom temperature in the secondary MOT on the frequency detuning δ of cooling radiation from resonance. Dashed line marks the Doppler temperature limit.

impedes laser cooling at small frequency detunings. To make the spectrum narrower, in future we will realise a scheme for stabilising the frequency of laser radiation relative to the reference resonator [32].

7. Optical dipole trap and one-dimensional optical lattice

We have demonstrated the process of re-capture of thulium atoms from the secondary MOT to the optical lattice [33] created by the radiation of a spatially single-mode, single-frequency Verdi V-10 laser (Coherent) with the wavelength $\lambda_0 = 532 \text{ nm}$ and power of 10 W focused to a spot with the diameter of $30 \mu\text{m}$ at the $1/e^2$ level. The dynamic polarisability of atoms at this wavelength is negative; hence, the atoms have a tendency to get into the domain with a maximal radiation intensity. The depth U of the corresponding potential well is approximately as follows [33]:

$$U = I \frac{3\pi c^2}{2} \sum_{\lambda} \frac{\lambda}{(2\pi c)^2} \Gamma_{\lambda} \left[\left(\frac{1}{\lambda} - \frac{1}{\lambda_0} \right)^{-1} + \left(\frac{1}{\lambda} + \frac{1}{\lambda_0} \right)^{-1} \right], \quad (5)$$

where I is the radiation intensity; and λ and Γ_{λ} are the wavelengths and probabilities of strong dipole transitions from the ground state in atom over which the summation is performed. With all transitions having the wavelengths from 400 to 1000 nm taken into account, the depth of dipole trap is several hundred microkelvins.

The laser radiation which forms the dipole trap was switched on during the whole cycle of measurements. Since the domain of existence for the dipole trap ($\sim 30 \mu\text{m}$) was substantially smaller than the dimension of the cloud in the MOT ($\sim 200 \mu\text{m}$) the presence of additional intensive radiation did not affected the efficient operation of the MOT. Atoms were loaded to the dipole trap in the following way. First, the secondary MOT was loaded then all laser beams were switched off. Atoms near the laser beam waist were subjected to the action of the dipole force that tended to localise them around the waist. Hence, if in a time interval much longer than the time of cloud expansion (see Fig. 4) the atoms are illuminated by a probe pulse of resonance radiation, then a cloud of the characteristic cigar shape will be detected which reproduces the shape of the Gaussian beam waist (Fig. 6a). If such a

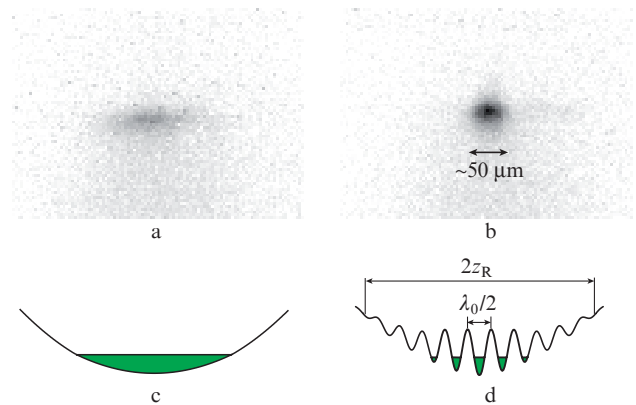


Figure 6. Photographs of atoms captured (a) in the dipole trap and (b) in the optical lattice; (c) schematic representation of the potential of the dipole trap and atoms in it; (d) schematic representation of the optical lattice with atoms [see (6)].

measurement is taken without a dipole trap, then as soon as in 7 ms after switching the laser beams off the cloud will greatly expand and the signal will be lost in noise (see Fig. 4).

A main drawback of the one-dimensional dipole trap is that it well localises atoms in the direction normal to the axis of laser beam [due to a small ($\sim 30 \mu\text{m}$) radius of the waist]; however, it badly localises atoms along the beam axis, because the Ray length z_R is several millimetres. This problem is solved by a one-dimensional optical lattice [33] produced by two counterpropagating focused beams of laser radiation of equal polarisations and frequencies. In such a configuration, a standing intensity wave is formed along the beam axis, which is equivalent to application to atoms a periodical potential which keeps them in the longitudinal direction, and the cloud captured to optical trap takes a more symmetrical shape (Fig. 6b). A distribution of radiation intensity and potential [see (5)] in the optical lattice have the form:

$$I(z, r) = 2I_0 \left(\frac{w_0}{w(z)} \right)^2 \exp \left(\frac{-2r^2}{w^2(z)} \right) \left[1 + \cos \left(2 \frac{2\pi}{\lambda_0} z \right) \right],$$

$$w(z) = w_0 \sqrt{1 + \left(\frac{z}{z_R} \right)^2},$$

$$z_R = \frac{\pi w_0^2}{\lambda_0},$$
(6)

where z is the coordinate along beam axis; r is the coordinate in the direction normal to the beam axis; $w_0 \sim 30 \mu\text{m}$ is the radius of the waist (at the intensity level $1/e^2$); $z_R \sim 2 \text{ mm}$ is the Ray length; I_0 is the intensity of each radiation beam forming the optical lattice; and $\lambda_0 = 532 \text{ nm}$ is the wavelength of light producing the optical lattice. The potential is schematically shown in Fig. 6d; its period is $\lambda_0/2$.

A part of atoms re-captured from the MOT to the dipole trap or optical lattice is only 1.5%. A small coefficient of re-capture is determined by the small ratio of a volume of the dipole trap to that of the cloud in the MOT, which is equal to $\sim 1\%$. The lifetime of atoms τ in the optical lattice was $320 \pm 50 \text{ ms}$ (Fig. 7). It is determined, most probably, by the losses of cooled atoms due to their resonance interaction with residual (i.e. passed through closed AOMs) laser radiation.

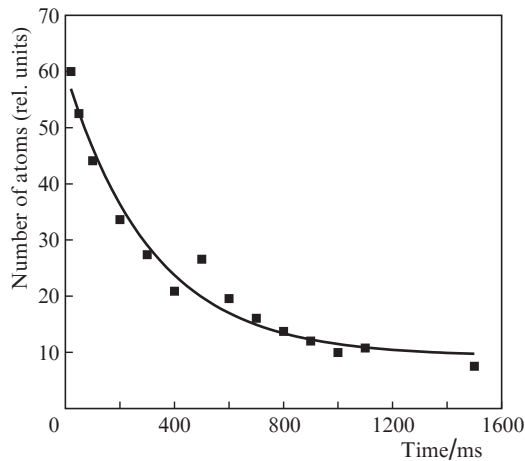


Figure 7. Kinetics of the number of atoms in the optical lattice.

8. Conclusions

We have demonstrated secondary laser cooling of thulium atoms and their capture by the MOT on the weak dipole transition $4f^{13}(^2F^o)6s^2, J = 7/2, F = 4 \rightarrow 4f^{12}(^3H_6)5d_{5/2}6s^2, J' = 9/2, F' = 5$ with the wavelength of 530.7 nm and natural linewidth of 350 kHz. The cloud in the secondary MOT comprised $10^4 - 10^6$ atoms having a temperature of 30–60 μK and lifetime of $2 \pm 0.1 \text{ s}$. We have realised the re-capture of atoms from the secondary MOT to a one-dimensional dipole trap and to the optical lattice produced by the laser radiation with a wavelength of 532 nm. The efficiency of re-capture was $\sim 1\%$ and the lifetime of atoms in the dipole trap was $320 \pm 50 \text{ ms}$.

To improve the signal/noise ratio in studying the metrological transition at the wavelength of 1.14 μm between components of the fine structure of the ground state in thulium atom, it is necessary to increase the number of atoms captured in the optical lattice by an order of magnitude by increasing the waist radius of the dipole trap and reducing the temperature of atoms in the MOT.

Acknowledgements. The work was financially supported by the Russian Foundation for Basic Research (Grant Nos 12-02-00867-a and 12-02-01374-a) and the Presidium of the Russian Academy of Sciences (Extreme Light Fields and Their Applications Programme).

References

- Andreev S.V., Balykin V.I., Letokhov V.S., Minogin V.G. *Pis'ma Zh. Eksp. Teor. Fiz.*, **34**, 463 (1981).
- Raab E.L., Prentiss M., Cable A., Chu S., Pritchard D.E. *Phys. Rev. Lett.*, **59**, 2631 (1987).
- Phillips W.D. *Rev. Mod. Phys.*, **70**, 721 (1998).
- Riehle F. *Frequency Standards. Basics and Applications* (Weinheim: Wiley-VCH, 2004).
- Weiner J., Bagnato V.S., Zilio S., Julienne P.S. *Rev. Mod. Phys.*, **71**, 1 (1999).
- Cronin A.D., Schmiedmayer J., Pritchard D.E. *Rev. Mod. Phys.*, **81**, 1051 (2009).
- Leggett A.J. *Rev. Mod. Phys.*, **73**, 307 (2001).
- Chou C.W., Hume D.B., Koelemeij J.C.J., Wineland D.J., Rosenband T. *Phys. Rev. Lett.*, **104**, 070802 (2010).
- Katori H. *Nature Photon.*, **5**, 203 (2011).
- Eschner J., Morigi G., Schmidt-Kaler F., Blatt R. *J. Opt. Soc. Am. B*, **20**, 1003 (2003).
- Katori H., Takamoto M., Pal'chikov V.G., Ovsyannikov V.D. *Phys. Rev. Lett.*, **91**, 173005 (2003).
- Hinkley N., Sherman J.A., Phillips N.B., Schioppo M., Lemke N.D., Beloy K., Pizzocaro M., Oates C.W., Ludlow A.D. *Science*, **341**, 1215 (2013).
- Kolachevsky N., Akimov A., Tolstikhina I., Chebakov K., Sokolov A., Rodionov P., Kanorski S., Sorokin V. *Appl. Phys. B: Las. Opt.*, **89**, 589 (2007).
- Kolachevsky N.N. *Usp. Fiz. Nauk*, **181**, 896 (2011) [*Phys. Usp.*, **54**, 863 (2011)].
- Ovsyannikov V.D. Private Communication.
- Berglund A.J., Lee S.A., McClelland J.J. *Phys. Rev. A*, **76**, 053418 (2007).
- Sukachev D.D., Sokolov A.V., Chebakov K.A., Akimov A.V., Kolachevsky N.N., Sorokin V.N. *Pis'ma Zh. Eksp. Teor. Fiz.*, **92**, 772 (2010) [*JETP Lett.*, **92**, 703 (2010)].
- Dalibard J., Cohen-Tannoudji C. *J. Opt. Soc. Am. B*, **6**, 2023 (1989).
- Frisch A., Aikawa K., Mark M., Rietzler A., Schindler J., Zupanič E., Grimm R., Ferlaino F. *Phys. Rev. A*, **85**, 051401 (2012).
- Berglund A.J., Lee S.A., McClelland J.J. *Phys. Rev. A*, **76**, 053418 (2007).
- Youn S.H., Lu M., Ray U., Lev B.L. *Phys. Rev. A*, **82**, 043425 (2010).

22. Hemmerling B., Drayna G.K., Chae E., Ravi A., Doyle J.M. arXiv:1310.3239 [physics.atom-ph] (2013).
23. Sukachev D., Sokolov A., Chebakov K., Akimov A., Kolachevsky N., Sorokin V. *Phys. Rev. A*, **82**, 011405 (2010).
24. Phillips W.D., Metcalf H. *Phys. Rev. Lett.*, **48**, 596 (1982).
25. Wickliffe M.E., Lawler J.E. *J. Opt. Soc. Am. B*, **14**, 737 (1997).
26. Letokhov V.S., Chebotaev V.P. *Printsipy nelineinoi lazernoi spektroskopii* (Principles of Nonlinear Laser Spectroscopy) (Moscow: Nauka, 1975).
27. Spedding F.H., Barton R.J., Daane A.H. *J. Am. Chem. Soc.*, **79**, 5160 (1957).
28. Chebakov K., Sokolov A., Akimov A., Sukachev D., Kanorsky S., Kolachevsky N., Sorokin V. *Opt. Lett.*, **34**, 2955 (2009).
29. Sukachev D.D., Kalganova E.S., Sokolov A.V., Savchenkov A.V., Vishnyakova G.A., Akimov A.V., Golovizin A.A., Kolachevsky N.N., Sorokin V.N. *Kvantovaya Elektron.*, **43**, 374 (2013) [*Quantum Electron.*, **43**, 374 (2013)].
30. Cohen-Tannoudji C., Dupont-Roc J., Grynberg G. *Atom – Photon Interactions: Basic Processes and Applications* (Weinheim: WILEY-VCH Verlag GmbH & Co. KGaA, 2004).
31. Kuhl J. *Zeitschrift für Physik*, **242**, 66 (1971).
32. Alnis J., Matveev A., Kolachevsky N., Wilken T., Udem Th., Haensch T.W. *Phys. Rev. A*, **77**, 053809 (2008).
33. Grimm R., Weidenmueller M., Ovchinnikov Y.B. *Adv. Atomic, Molec. Opt. Phys.*, **42**, 95 (2000).